Stochasticity and Intramolecular Redistribution of Energy

edited by

R. Lefebvre
Laboratoire de Photophysique Moléculaire du CNRS,
Orsay, France

and

S. Mukamel
Department of Chemistry, University of Rochester,
New York, U.S.A.

D. Reidel Publishing Company

Dordrecht / Boston / Lancaster / Tokyo

Published in cooperation with NATO Scientific Affairs Division

Proceedings of the NATO Advanced Research Workshop on
Stochasticity and Intramolecular Redistribution of Energy
Orsay, France
June 23 - July 4, 1986

Library of Congress Cataloging in Publication Data

NATO Advanced Research Workshop on Stochasticity and Intramolecular Redistribution of Energy (1986: Orsay, France)
Stochasticity and intramolecular redistribution of energy.

(NATO ASI series. Series C, Mathematical and physical sciences; vol. 200)
Includes index.
1. Excited state chemistry—Congresses. 2. Stochastic processes—Congresses. I. Lefebvre, R. (Roland), 1928– . II. Mukamel, S. (Shaul), 1948– . III. Title. IV. Series.
QD461.5.N357 1986 541.2'24 87–4598
ISBN 90–277–2462–8

Published by D. Reidel Publishing Company
P.O. Box 17, 3300 AA Dordrecht, Holland

Sold and distributed in the U.S.A. and Canada
by Kluwer Academic Publishers,
101 Philip Drive, Assinippi Park, Norwell, MA 02061, U.S.A.

In all other countries, sold and distributed
by Kluwer Academic Publishers Group,
P.O. Box 322, 3300 AH Dordrecht, Holland

D. Reidel Publishing Company is a member of the Kluwer Academic Publishers Group

Printed in The Netherlands

CONTENTS

DOPPLER FREE EXCITATION OF LARGE MOLECULES AND NONRADIATIVE DECAY OF INDIVIDUAL LEVELS

E. Riedle and H. J. Neusser
Institut für Physikalische und Theoretische Chemie
Technische Universität München
Lichtenbergstr. 4
D-8046 Garching, West Germany

ABSTRACT. Doppler-free two-photon spectroscopy with cw and pulsed Fourier transform limited light sources allows the resolution of the rotational structure of the electronic spectrum of large molecules. Besides a very detailed analysis of the spectrum and a precise determination of spectroscopic constants, the observation of the decay behavior of individual levels is made possible in this way. Examples are presented for the prototype molecule benzene, C_6H_6. While regular behavior prevails in the 14^1_0-band at low vibrational excess energy, it is shown that strong coupling to background states occurs in the $14^1_0 1^1_0$-band at intermediate excess energy. A detailed model for this coupling is presented.

1. INTRODUCTION

Ever since the first observations of nonradiative decay in large molecules, the question of the dependence of the decay rate on the excess energy in the electronic state and the nature of the states excited has been the topic of numerous investigations /1/. Generally, an increase in the nonradiative decay rate with excess energy is observed which may be quite dramatic as in the case of the onset of the so called "channel three" in benzene /2,3/.

The excitation of single vibronic states is found to be nontrivial in room temperature gas phase studies of large molecules that can display nonradiative decay, due to the rotational inhomogeneous broadening and the presence of sequence bands in the spectrum. Experiments in supersonic jets with their extremely low rotational temperature allowed great progress in this respect in the last few years, however, at the expense of loss of knowledge about the influence of the molecular rotation on the decay behavior.

R. Lefebvre and S. Mukamel (eds.), Stochasticity and Intramolecular Redistribution of Energy, 203–216.

All decay time measurements made so far /4/ have been selecting bunches of rovibronic states with a common vibronic identity rather than single rovibronic states. In recent years, however, there have been some indications from moderately resolved measurements, that the decay behavior may vary over the rotational contour of a vibronic transition /5/. This makes it desirable to observe the decay of single rovibronic states. For the large molecules that show nonradiative decay this is not easily done. Doppler-broadening in the gas phase makes the resolution of single lines in the spectrum impossible, since many rotational lines are located within the Doppler width. With the advent of tunable, narrow band, high power laser light sources a number of Doppler-free techniques /6/ like spectroscopy in a collimated molecular beam, saturation and polarization spectroscopy and Doppler-free two-photon spectroscopy became available. These methods were first successfully applied in atomic physics but now they are also used in molecular spectroscopy /7/. In this contribution we will show that Doppler-free two-photon spectroscopy allows the complete resolution of the rotational line structure of vibronic bands of the large prototype molecule benzene and the investigation of the nonradiative decay of individual rovibronic levels.

2. EXPERIMENTAL TECHNIQUES

The experimental set up used for the recording of Doppler-free two-photon spectra and the investigation of the decay of individual levels has been described in detail previously /8,9/. Only a brief review will be given here.

Doppler-free excitation takes place if a molecule simultaneously absorbs two photons of equal energy and opposite direction of propagation from a standing wave light field /10/. Such a light field can be generated by reflecting a laser beam back into itself or it exists inside a cavity, for example a Fabry-Perot resonator. The laser light used has to be extremely narrow band since the experimental resolution that can be obtained is limited by this frequency width. In our experiments the light of a cw frequency stabilized single mode ring dye laser (CR 699/21) pumped by a Kr^+ laser is used. At a wavelength around 5000 A typically 250 mW of tunable light with a frequency width (FWHM) of 1 MHz are available. For extremely high spectral resolution and very high sensitivity the Doppler-free experiment is performed within a concentric external cavity whose length is locked to the laser frequency /8/. The UV-fluorescence following the excitation of the molecules is monitored by single photon counting. The use of the external cavity

increases the sensitivity by two orders of magnitude as compared to the simpler arrangement of the backreflected laser beam. A resolution of better than 10 MHz can be obtained with this cw set up /8/.

For the investigation of the decay of individual levels pulsed excitation of the molecules has to be used. The experimental set up is shown in Fig. 1 /9/. Extremely narrow band pulsed laser light is produced by pulsed amplification of the cw light. With three stages of excimer laser pumped amplifiers we can generate light pulses of 500 KW peak power and nearly Fourier transform limited bandwidth. With an additional parasitic cavity around the second amplifier the pulse length can be varied between 2.5 ns and 10 ns and the frequency width accordingly between 50 MHz and 180 MHz. After passing through the sample cell the laser beam is reflected back into itself to allow the Doppler-free absorption. The two beams are counterclockwise circularly polarized to suppress the Doppler-broadened background /11/. The resulting UV-fluorescence signal is either integrated for the recording of spectra or its time behavior is recorded with a transient digitizer. It is worth mentioning that in Doppler-free two-photon absorption all molecules regardless of their velocity contribute to the observed signal. Molecules are only excited to one single level if the laser frequency is set to a resolved rotational line in the spectrum regardless of the number of lines within the Doppler width. This allows the observation of the decay of an individual level /9/.

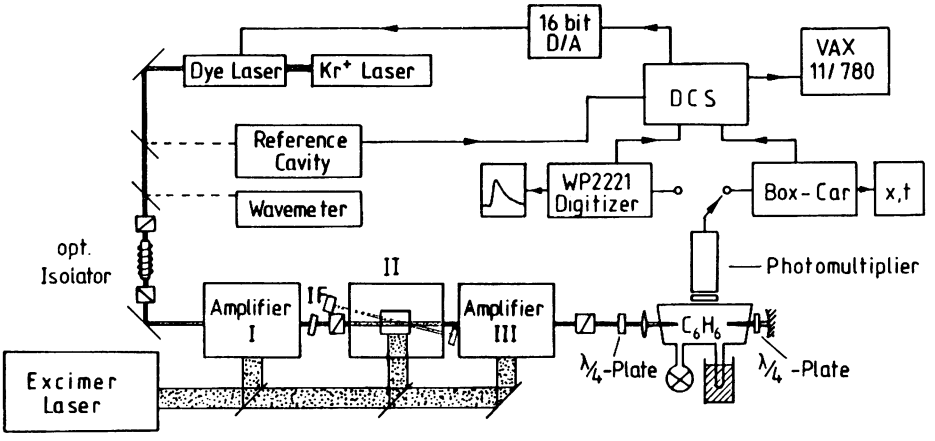

Figure 1. Experimental set up for decay time measurements of individual rotational levels of S_1 benzene. Fluorescence decay is observed after pulsed Doppler-free two-photon excitation with the amplified light of the cw laser.

3. EXPERIMENTAL RESULTS AND DISCUSSION

3.1. 14^1_0-Band of C_6H_6, typical for low excess energy

3.1.1. Spectroscopic results The first 6 cm^{-1} of the Doppler-free spectrum of the Q-branch of the 14^1_0-band of benzene, C_6H_6, at 39656.90 cm^{-1} are shown in Fig. 2. The spectrum has been recorded with a sample pressure of 0.7 Torr in our cw set up. The lines observed in the spectrum correspond to well resolved single rotational lines. The Doppler-width of 1.7 GHz would not allow the resolution of the individual rovibronic transitions since typically 10 lines are located within the Doppler-width. All lines in the spectrum in Fig. 2 can be assigned within the model of a semirigid symmetric top. A fit to the observed line posi-

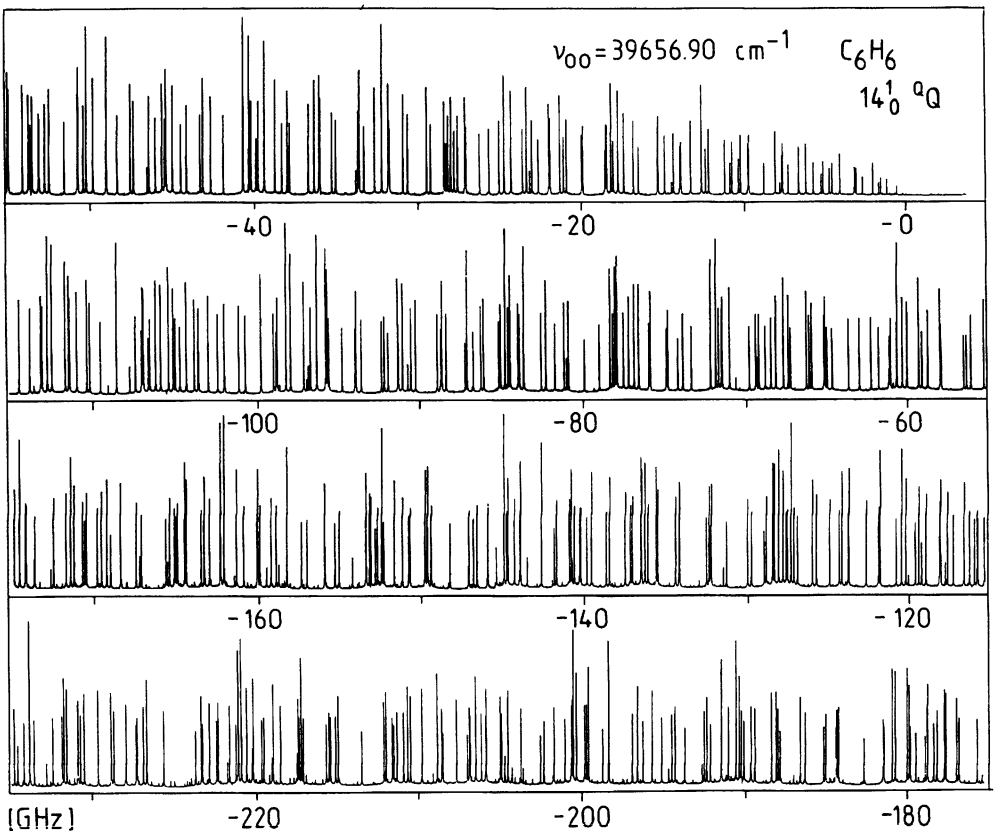

Figure 2. Part of the Doppler-free room temperature spectrum of the Q-branch of the 14^1_0-band of benzene, C_6H_6. Every line corresponds to an individual rovibronic transition. All of the lines have been assigned.

tions renders the rotational constants of the excited state with an accuracy of 10^{-7} cm^{-1} and the quartic centrifugal distortion contants with an accuracy of 10^{-10} cm^{-1} /13/. This accuracy is higher by two orders of magnitude than previously obtained with Doppler-limited spectroscopy. The remaining deviations (residuals) between the calculated line positions and the observed ones are about 10 MHz. These results clearly show that Doppler-free two-photon spectroscopy allows the complete resolution of the electronic spectrum of benzene and the spectrum is extremely well reproduced with the simple model of a semirigid symmetric top.

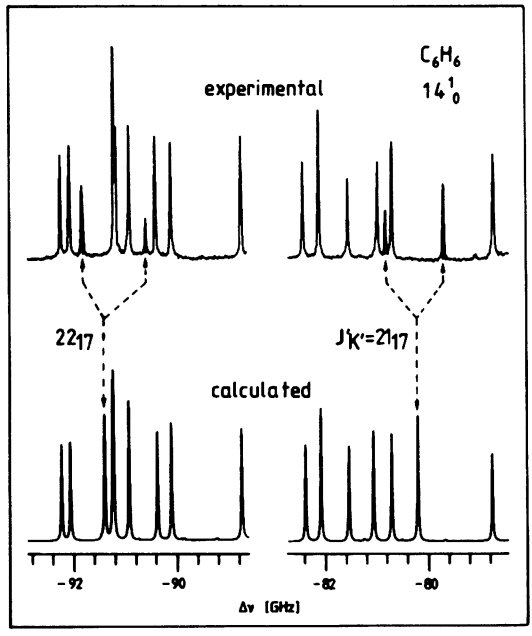

Figure 3. Two small parts of the Q-branch of the 14^1_0-band under Doppler-free resolution. Upper traces: measured spectra; lower traces: calculated spectra. Instead of the predicted peaks $J'_{K'}=21_{17}$ and $J'_{K'}=22_{17}$ two peaks appear shifted from the calculated position in each case. (taken from ref. /14/.)

In some parts of the spectrum, at higher rotational energy differences between the experimental spectrum and the calculated one are observed. This is shown for two examples in Fig. 3. While most of the observed lines (top part of Fig. 2) are well reproduced by the calculation (bottom part of Fig. 3) single lines of the calculated spectrum are not found in the experimental one /14/. Instead two smaller lines are observed in each case. If these pairs of

lines are labeled with the rotational quantum numbers of the missing lines the dependence of the deviations on the quantum number J of total angular momentum can be plotted for each value of K, where K is the quantum number of the projection of $\vec{J}$ on the figure axis of the molecule. The result is shown in Fig. 4. The typical J-dependence of the deviations found is that of an avoided crossing. A careful analysis shows /14/ that the observed perturbations are caused by the coupling of light rotational states of the 14^1 vibronic state to dark rovibronic states in the electronic S_1 state. As a result two eigenstates with mixed vibronic character result and both can be seen in the spectrum. These are the two lines observed in the experimental spectrum as indicated in Fig. 3. From the positions of the two lines the coupling matrix element can be calculated for each pair /13/. The coupling shows a strong dependence on J and K. This leads to the conclusion that the observed coupling must be caused by perpendicular Coriolis coupling rather than by anharmonic or parallel Coriolis coupling /13/.

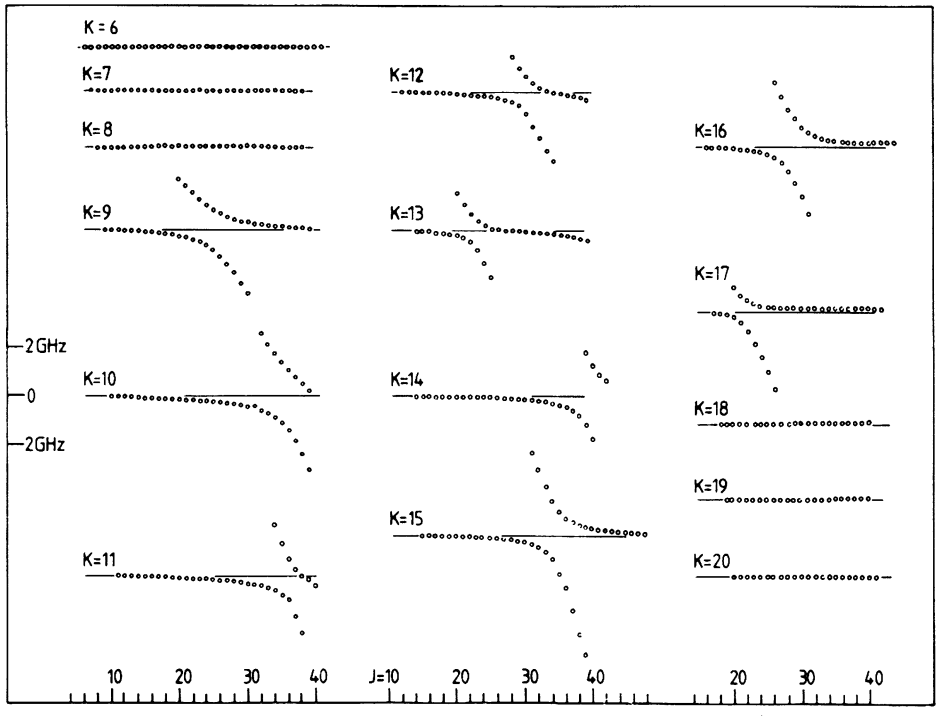

Figure 4. Residuals (calculated - observed) of the frequencies of rotational lines in the spectrum of the 14^1_0-band as a function of the final state quantum number J' for several values of K'.

3.1.2. Decay behavior of individual levels With the pulsed set up individual rotational levels in the 14^1 vibronic state can be populated and their decay behavior observed under collisionless conditions /9/. For all states that were found unperturbed in the spectroscopic analysis a single exponential decay is found and the decay time of τ=135 ns is independent of the rotational quantum numbers J and K. This is in good agreement with the assumption that the decay of the levels is determined by the radiative decay and more strongly by the coupling to the T_1 triplet state in the statistical limit /15/. On the contrary, for states found to be perturbed a significantly shorter decay time is found /9/. For example, the $J_K=(24_9)_a$ state resulting from the coupling of the $J_K=24_9$ rotational state of the 14^1 vibronic state to a dark rovibronic state has a decay time of only 87 ns. The decay is again single exponential. It can be concluded that the dark zero order state decays much faster and due to the mixed vibronic nature of the observed eigenstate its shorter decay time results. It is seen that there exist vibrational states in S_1 at the vibrational excess energy of the light state that possess much faster decay rates. These states can not be directly excited and their observation is only possible through the analysis of perturbations. It will turn out that the existence of shortlived background states is important for the interpretation of observations at higher excess energy that are discussed below.

3.2. $14^1{}_0 1^2{}_0$-Band of C_6H_6, typical for intermediate excess energy

The nonradiative decay rate of S_1 states generally increases with vibrational excess energy. This increase is found to be fairly slow in benzene for energies below 3000 cm^{-1} but at about this energy a sudden strong decrease of the fluorescence quantum yield was found from low resolution experiments /15/. It is accompanied by the indication of severe broadening in the absorption spectrum /2/. Since none of the known radiative and nonradiative decay channels of benzene was believed to explain this behavior, it was attributed to an unknown "channel three" /2/. None of the Doppler limited measurements was able to resolve the rotational structure of the vibronic bands and therefore no information on the rotational dependence of "channel three" was available from the above mentioned experiments.

Doppler-free two-photon spectra in the vicinity of the onset of "channel three" can be recorded for progression and sequence bands of the $14^1{}_0$-band discussed above. For a progression band the rotational structure should be iden-

tical to that of the fundamental band except for small changes in the exact positions of the rotational lines due to small changes in the rotational constants. This is for example the case for the 14^1_0-band (at 1571 cm^{-1} excess energy) and the $14^1_0 1^1_0$-band (2492 cm^{-1}). The transitions of both bands lead to states below the onset of "channel three". On the contrary, the upper state of the $14^1_0 1^2_0$-band is the $14^1 1^2$ state at 3412 cm^{-1} just above the onset of the postulated "channel three". A precise analysis of this band should therefore render important information about the origin of the fast nonradiative decay.

3.2.1. Disappearance of rotational lines The Doppler-free spectrum of the blue edge of the Q-branch of the $14^1_0 1^2_0$-band is shown in Fig. 5 /8/. This spectrum was measured with the cw set up at a resolution of about 15 MHz. The spectral range shown and the frequency scale is identical with the part of the 14^1_0-band shown at the top of Fig. 2. A comparison of the two spectra immediately shows that most of the rotational lines are missing in the $14^1_0 1^2_0$-band /8,16/. To understand this surprising result

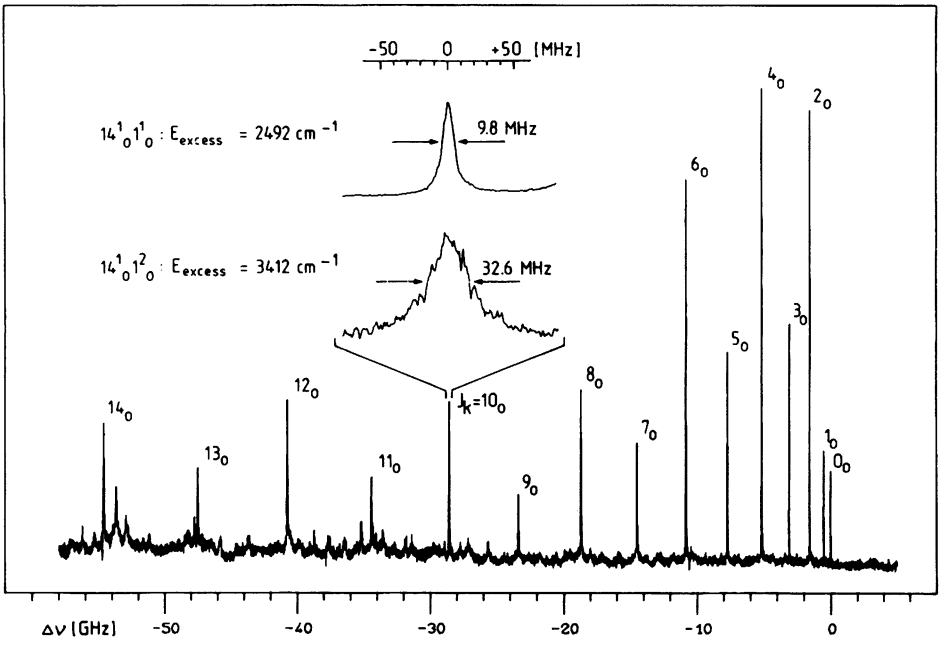

Figure 5. Part of the Doppler-free two-photon spectrum of the $14^1_0 1^2_0$-band of C_6H_6 (taken from ref. /8/). The lineshapes of the $J_K=10_0$ line of the $14^1_0 1^1_0$-band and the $14^1_0 1^2_0$-band are shown on an expanded scale.

it has to be kept in mind that the Doppler-free spectra reported are not absorption spectra but fluorescence excitation spectra. The two kinds of spectra would be identical if the fluorescence quantum yield were identical for all states excited. For this reason the disappearance of lines in the $14^1_0 1^2_0$-band is interpreted as a lack of fluorescence from the states populated, i.e. a fast rotationally dependent nonradiative decay.

From the position of the lines and the alternating intensity the remaining lines in the spectrum of the $14^1_0 1^2_0$-band were identified as K=0 lines /16/. From the disappearance of the K≠0 states we concluded that they are coupled to dark background states that rapidly decay. The coupling was identified as parallel Coriolis coupling with strength proportional to K /16/.

3.2.2. Homogeneous linewidths and decay time measurements of K=0 states The extremely high resolution of the cw set up allows the measurement of homogeneous linewidths at very low sample pressure /8/. If the homogeneous linewidth of identical rotational lines from the $14^1_0 1^1_0$-band and the $14^1_0 1^2_0$-band are compared, a significant increase in linewidth is found for the $14^1_0 1^2_0$-band. This is shown for the $J_K=10_0$ line in the inserts of Fig. 5. While the linewidth is still experimentally limited for the $14^1_0 1^1_0$-band, homogeneous linewidths were measured for K=0 lines in the $14^1_0 1^2_0$-band for different J values /8/. These are found to increase from 2 MHz for J=0 to 46 MHz for J=14. All the observed lines have a Lorentzian lineshape within experimental accuracy.

The pulsed set up allows the measurement of decay curves for the same states (K=0) in the $14^1 1^2$ vibrational state /12/. For the states with low J value pulses whose width is close to 10 ns were used to ensure the highest possible resolution while for higher J values pulses of 2.5 ns duration allowed the resolution of fast decays. Typical results are shown in Fig. 6. All decay curves are single exponential and the decay times range from $\tau \geq 55$ ns for J=0 to $\tau = 7.1$ ns for J=8. The observed decay rates closely agree with the relaxation rates obtained from the linewidth measurements discussed above.

The strong dependence of the decay rate on J can not be due to a rotational dependence of the pure electronic radiative or nonradiative decay rate of the $14^1 1^2$ state since such a dependence was not found for the 14^1 state and for this reason is not expected for the $14^1 1^2$ state either. Instead it has to be interpreted as a rotationally dependent IVR process which mixes the optically light state with

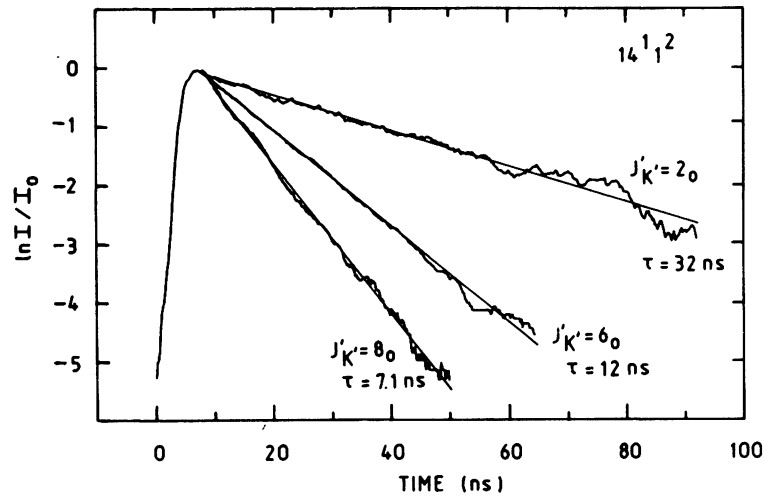

Figure 6. Decay curves for K=0 rotational states (differing in J) of the $14^1 1^2$ vibronic state of C_6H_6 (taken from ref. /12/).

dark states in S_1 that rapidly decay nonradiatively. From the exact J dependence seen the underlying responsible coupling process is found to be perpendicular Coriolis coupling /8,12/.

3.2.3. Model for the observed coupling in the $14^1 1^2$-state

From the experimental results reported above a model for the coupling of the $14^1 1^2$-state and its relaxation behavior evolves that is shown systematically in Fig. 7. The rotational states ($0 \leq J \leq 14$) of the $14^1 1^2$ vibronic state (shown in the middle of Fig. 7) are coupled to the rotational states of two different dark vibrational states in S_1 by different coupling mechanisms. Parallel Coriolis interaction leads to a coupling with a vibrational state of b_{1u} symmetry (shown in the right part of Fig. 7) and perpendicular Coriolis interaction leads to a coupling with a vibrational state of e_{2u} symmetry (shown in the left part of Fig. 7). The background states themselves are strongly coupled to the quasicontinuum of vibrational states in the S_0 and/or T_1 electronic state and therefore decay very fast and show strong broadening /17/. The probable reason for this strong coupling is that the dark background states are combination states containing quanta of out of plane modes /8,12,16/. These modes are the lowest frequency modes in benzene and are contained with a high probability

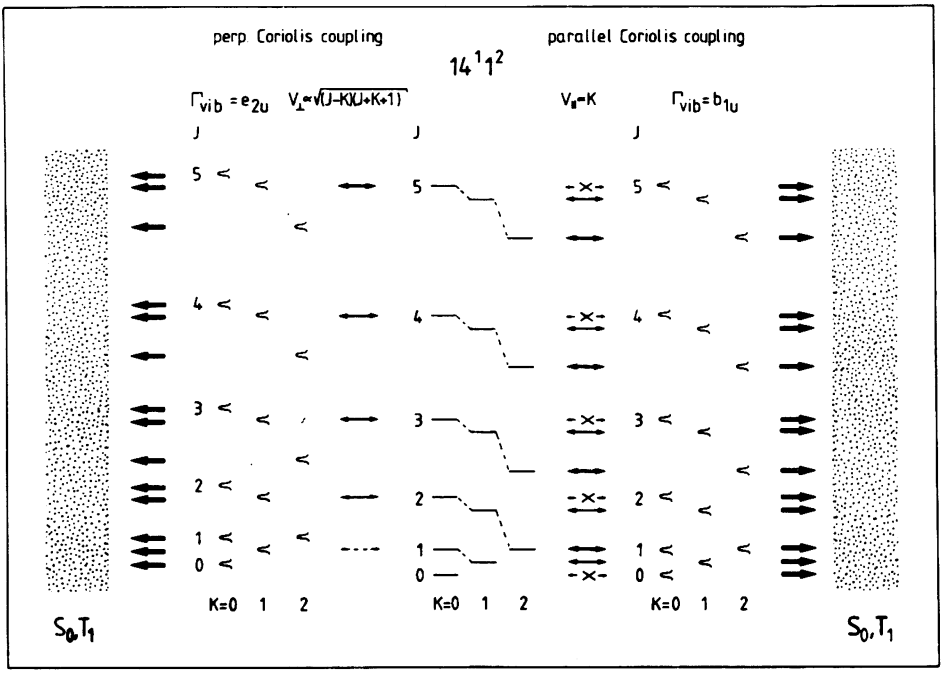

Figure 7. Schematic representation of the coupling of the low J,K rotational states of the $14^1 1^2$ vibronic state of C_6H_6 (middle part) to dark broadened states in S_1 (outer parts). The coupling is due to parallel Coriolis coupling (right part) and perpendicular Coriolis coupling (left part).

in the background states at the excess energy of 3412 cm^{-1}. They are known to strongly increase the nonradiative decay of a state as they are good accepting modes /18/. The eigenstates that result from the mixing with the rapidly decaying dark background states therefore decay themselves very rapidly. Their fluorescence quantum yield is very low and the K≠0 lines are not seen in the spectrum. K=0 lines are not affected by this coupling since the strength of parallel Coriolis coupling is proportional to K. Due to the $\Delta J, \Delta K = 0$ selection rule of parallel Coriolis coupling /19/ the resonance condition for the coupling is automatically fullfilled for all states with different J and K if there exists a single vibrational background state at resonance with the $14^1 1^2$ zero order state. Only for very high J,K states the resonance condition is lost due to the slightly differing rotational constants of both coupled states. This is indeed observed for J > 14 and a different strong coupling process (perpendicular Coriolis coupling) is active in this range of the spectrum /8/.

The second coupling mechanism in the low J range is weaker and only seen for the remaining K=0 states. These states are supposed to be in additional resonance with the rotational states of a vibrational state of e_{2u} symmetry (shown in the left part of Fig. 7) which are again strongly broadened due to the reasons discussed above. The pairs of states are coupled by perpendicular Coriolis coupling which for K=0 is proportional to $\sqrt{J(J+1)}$ /19/. This causes a J dependent mixing of the states and explains the observed J(J+1) dependence of the decay rate of the K=0 states (see Fig. 6) /8,12/.

4. SUMMARY AND CONCLUSION

Doppler-free two-photon spectroscopy is shown to allow the resolution of individual rotational lines in the electronic spectrum of large molecules. This result is demonstrated for the prototype molecule benzene.

In the low excess energy regime the rotational spectrum can be explained with a simple semirigid symmetric top Hamiltonian. Isolated perturbations can be explained by the selective coupling of the light states to dark S_1 states. This coupling causes a mixing of the zero order states and makes both resulting eigenstates observable. This permits the characterization of the dark state and its decay behavior.

Above the onset of the postulated "channel three" (in the $14^1_0 1^2_0$-band) most rotational lines are missing. From the analysis of the spectrum and from linewidth and lifetime measurements a detailed model about the relaxation of the different states is found. It is concluded that rotational dependent intramolecular vibrational redistribution (IVR) induced by Coriolis coupling is the primary process for the nonradiative decay of the $14^1 1^2$-state. Other vibrational states in the same excess energy range will be affected in a similar way, however, the exact appearance of the vibronic bands will depend on the accidental positions of states, the strength of the coupling matrix elements and the selection rules of the particular coupling mechanism active. The analysis of many bands and different molecules with the Doppler-free high resolution technique presented in this work /20/ should allow the complete understanding of the nonradiative behavior of large molecules and in particular of the "channel three" phenomenon of benzene.

The results presented show the importance of rotation for the nonradiative decay of large molecules. As the rotational structure of the electronic spectrum can only be

resolved by Doppler-free techniques, Doppler-free spectroscopy is seen to be of great importance for an exact understanding of nonradiative decay.

5. ACKNOWLEGEMENT

We wish to thank Prof. Dr. E. W. Schlag for his contributions to the results presented in this paper. Valuable experimental support by H. Stepp, U. Schubert and H. Sieber is greatfully acknowledged.

REFERENCES

1. For a review see, K. F. Freed in: Topics in Applied Physics, ed. F. K. Fong, Vol. 15, p. 23 ff., Springer, Berlin, 1976

2. J. H. Callomon, J. E. Parkin, and R. Lopez-Delgado, Chem. Pys. Lett. 13, 125 (1972)

3. L. Wunsch, H. J. Neusser, and E. W. Schlag, Z. Naturforsch. Teil A 36, 1340 (1981)

4. Compare for example: K. G. Spears and S. A. Rice, J. Chem. Phys. 55, 5561 (1971); L. Wunsch, H. J. Neusser, and E. W. Schlag, Chem. Phys. Lett. 32, 210 (1975); M. Sumitani, D. V. O'Connor, Y. Takagi, N. Nakashima, A. Kamagawa, Y. Udagawa, and K. Yoshihara, Chem. Phys. 93, 359 (1985)

5. B. E. Forch, K. T. Chen, H. Saigusa, and E. C. Lim, J. Phys. Chem. 87, 2280 (1983); P. M. Felker and A. H. Zewail, J. Chem. Phys. 82, 2994 (1985); A. Amirav and J. Jortner, J. Chem. Phys. 84, 1500 (1986)

6. For a review see, W. Demtröder, "Laser Spectroscopy", Springer, Berlin, 1981

7. E. Riedle, H. J. Neusser, and E. W. Schlag, J. Chem. Phys. 75, 4231 (1981); K. H. Fung and D. A. Ramsay, J. Phys. Chem. 88, 395 (1984); A. Kiermeier, K. Dietrich, E. Riedle, and H. J. Neusser, J. Chem. Phys., in press

8. E. Riedle and H. J. Neusser, J. Chem. Phys. 80, 4686 (1984)

9. U. Schubert, E. Riedle, and H. J. Neusser, J. Chem. Phys. 84, 5326 (1986)

10. L. S. Vasilenko, V. P. Chebotayev, and A. V. Shishaev, JETP Letters 12, 113 (1970)

11. E. Riedle, R. Moder, and H. J. Neusser, Opt. Commun. 43, 388 (1982)

12. U. Schubert, E. Riedle, H. J. Neusser, and E. W. Schlag, J. Chem. Phys. 84, 6182 (1986)

13. E. Riedle and H. J. Neusser, in preparation

14. E. Riedle, H. Stepp, and H. J. Neusser, Chem. Phys. Lett. 110, 452 (1984)

15. For a review see, C. S. Parmenter, Adv. Chem. Phys. 22, 365 (1972)

16. E. Riedle, H. J. Neusser, and E. W. Schlag, J. Phys. Chem. 86, 4847 (1982)

17. A. Nitzan, J. Jortner, and P. M. Rentzepis, Proc. R. Soc. London Ser. A 327, 367 (1972); F. Lahmani, A. Tramer, and C. Tric, J. Chem. Phys. 60, 4431 (1974)

18. H. Hornburger and J. Brand, Chem. Phys. Lett. 88, 153 (1982)

19. I. M. Mills, Pure Appl. Chem. 11, 325 (1965)

20. Compare for example recent measurements by our group, for which a theoretical interpretation is presented by S. F. Fischer and W. Dietz in this volume

SUBJECT INDEX

A

B

C

R

S

T

U

V

W

Z